GeoAmericas2020
4th PAN AMERICAN CONFERENCE ON GEOSYNTHETICS
26-29 APRIL 2020 • RIO DE JANEIRO • BRAZIL

Analysis of the Shear Stress Distribution on the Interface Shear Test for a Texturized Geomembrane and Gold Mining Underflow

Ana L. M. Halabi, Department of Geotechnical and Transportation Engineering of the University of Minas Gerais, Belo Horizonte, Brazil
K. Pimentel, Department of Geotechnical and Transportation Engineering of the University of Minas Gerais, Belo Horizonte, Brazil
M.G. Gardoni, Department of Geotechnical and Transportation Engineering of the University of Minas Gerais, Belo Horizonte, Brazil
S.S. Sampaio, DAM, Belo Horizonte, Brasil

ABSTRACT
Geosynthetic polymeric barriers has been used in the impermeabilization of tailings dams, but causes concern regarding its performance under high loadings, especially in the interface with the dam and the foundation, due to the possibility of a low resistance or high deformability plane. Therefore, the interface between the dam material, underflow of tailings from a gold ore mining, and a texturized 1,5 mm HDPE geomembrane was evaluated numerically, using the finite element software RS2, in an interface shear test. It was observed that the interface did not respond to the elastic-plastic behavior and that therefore Mohr-Coulomb yielding criteria did not represent well the behavior of the experimental curve during shear. It was also observed the sensibility of the model to the loadings. The influence of the boundary conditions in the presented simulation also needs to be evaluated and probably better discretized.

1. INTRODUCTION

Tailings dams are large structures responsible for the storing of the residues from the mining industries and, therefore, needs to accommodate displacements due to the various external and internal loads (Acosta et al., 2018). For the gold ore tailings dam, impermeabilization liners are used for safety and environmental impacts reduction due to the toxic substances, like heavy metals and other pollutants diluted in its water, and the need to preserve the surrounding soil and underground water. However, this material can represent a major factor on the structure's stability. potential rupture surface and

Among the waterproofing barriers, the HDPE is currently widely used in landfills to foreclose liquids and gases, and its use in the mining industry is currently increasing. The design of these liners in the mining industry however, need to consider the high stress levels they are subjected to, and its effects on the geomembrane liner, as well as the liner bedding and the drainage layers (Lupo & Morrinson, 2007). Its use in tailings dams is also still limited due to the little capacity these materials have to adapt to large deformations, due to its rigidity (Sampaio, 2013).

The choice of using a geomembrane, however, could induce the existence of a failure or sliding surface passing through the interface, which could influence the dam's stability. This could be an important factor on its stability since it impacts the development of deformations, wrinkles and defects (Power, et al., 2017) due to the possibility that the interface between the underflow and the geomembrane presents low shear resistance or high deformability (Sampaio, 2013). Thus, it is necessary to analyze the dam's stability to this potential failure mode.

Therefore, other than the stability analysis, it is also important to evaluate the performance of the dam when submitted to on-site deformation, usually done by numerical strain-stress analysis. It is also important to evaluate the performance of the liner interface, since its deformations could cause cracks, that could become a favourable water path and, therefore, cause internal erosion or an slippage surface due to its weakness (Yaya, et al., 2017). Making an analogy between the stress distribution on the liner interface and a soil reinforced with geosynthetic, we could predict that the deformation response of the structure comes from the shear strength properties of the soil, the geosynthetics tensile properties and the stress transfer between it and the soil (Teixeira, et al., 2007).

Therefore, this work presents a study of the behavior of the geomembrane-underflow interface of a gold ore tailings dam. For that, it was performed a numerical simulation of an interface direct shear test, conducted by Sampaio (Sampaio, 2013), in order to study the behavior of the interface under axial loading and adjust the modeling of the geomembrane and its interface with the underflow. The data used corresponds with one of the sections of a gold ore tailings dam in Brazil, in which, the foundation was impermeabilized with a 1.5 mm texturized HDPE geomembrane. Finally, there are presented the conclusions of this research and suggestions for future research.

2. THE GOLD ORE TAILINGS DAM

The tailings dam of this study is being built by the downstream method. Its reservoir, its foundation, and its upstream slope were impermeabilized with a 1.5 mm texturized HDPE geomembrane, in order to prevent the contamination of the aquifer and the soil. Fig. 1a presents the details of the impermeabilization system at the foot and Fig 1b) at the top of the upstream slope.

2.1 Geotechnical Parameters of the Materials

The cross-section of the dam studied is presented in Fig. 2. The main materials and components of the cross-section of the studied dam are the tailings deposited in the reservoir, the cycloned tailings or underflow, of which the dam is built, with a compaction degree of 90% for lower stages of construction and of 95% for newer stages of construction, borrowed clay material, the drain, the starting dam, and the waterproofing 1.5 mm texturized HDPE geomembrane. The geotechnical parameters of the construction materials of the dam and the geomembrane-underflow interface were obtained from the results presented for laboratory tests performed by Sampaio (Sampaio, 2013). Table 1 presents the values of the effective resistance parameters of the constituent materials, considered as medium parameters for the analysis in this paper.

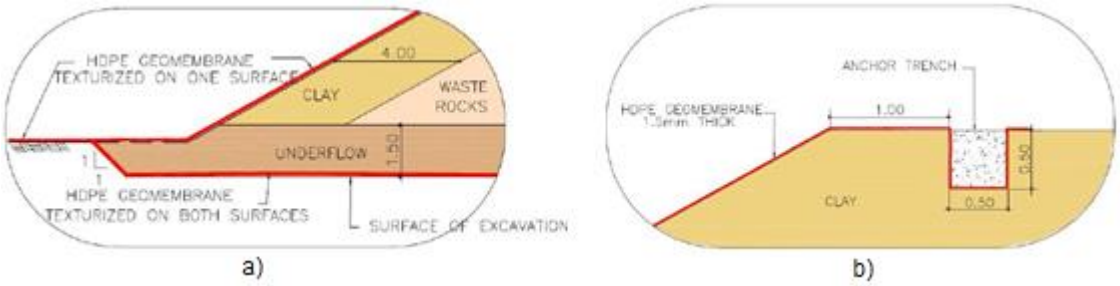

Fig. 1. Detailing of the Geomembrane's Placement a) in the Upstream's Slope Foot and b) in the Upstream's slope top (Sampaio, 2013)

Table 1. Geotechnical Parameters (Sampaio, 2013) Modified

Materials	**γ (kN/m3)**	**c' (kN/m2)**	**ϕ (°)**
foundation	20	40	32
tailings	20	0	26
underflow-geomembrane interface	-	0	28
underflow 90%	22	0	30
underflow 95%	22	0	36
clayey soil	20	16	31
drain	20	0	30
started dike	20	20	28

3. NUMERICAL MODELLING

In this item it is presented the results of the strain-stress analyses coming from the numerical simulations of interface shear test for three different axial confining tensions. It was analyzed the geometry and the boundary conditions of the problem as well as the use of constitutive models' representatives of the materials utilized.

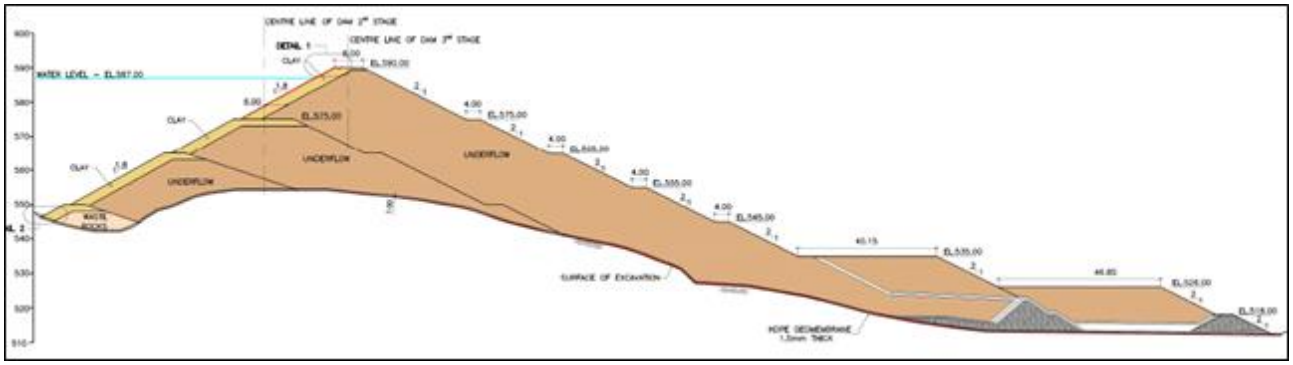

Fig. 2. Cross Section of the Dam in the Third Stage (Sampaio, 2013).

3.1 Geometry of the Computational Model

For a future evaluation of the interface performance under the effect of the dam's weight, it was performed a numerical simulation for the interface shear test. Aspects relative to the geometry and the boundary conditions were evaluated, as well as the constitutive models representatives of the materials utilized.

The boundary conditions for the interface shear test were considered accordingly to the tests described by Sampaio et al. (2017). The tests were conducted using standardized equipment used for direct shear tests, whose box has internal dimensions of 10cm x 10cm in plant and 2cm of height. It was also used a 1.5 mm t HDPE geomembrane texturized in both sides. In the test, in order to guarantee that the rupture occurred in the geomembrane-underflow interface, steel plates were inserted in the lower rigid base of the shear cell, over which the geosynthetic were glued with silicone to avoid wrinkling. The gold ore tailings were, then, molded in the upper piece of the shear cell, with a height of 1 cm.

The specimen was submitted to a punctual confining load, normal to the shear box, in a rigid surface that distributed the loading to the sample. The test was then carried out by applying a constant displacement to the lower portion of the box relative to the upper box of the equipment, which is kept still due to displacement restrictions. Fig. 3 illustrates the mechanical press of ELE International, used by Sampaio (2013) to perform the tests. In this diagram stands out that the sheer tension is calculated by the reaction force in the dynamometric ring, and from its relation with the corrected area of the surface, the medium shear stress in the sliding surface is determined.

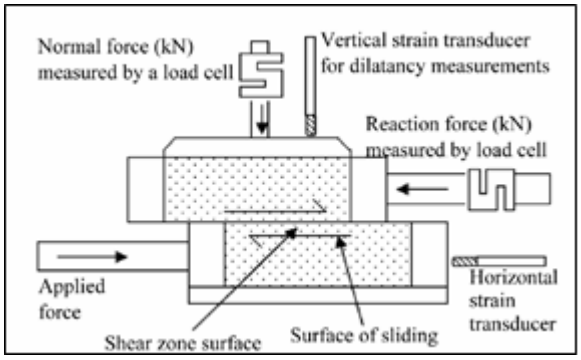

Fig. 3. Scheme of a Direct Shear Box Test (Wijeyesekera, et al., 2013)

For the computational model, the displacements restriction in the superior shear box was simulated with supports that restricts the movement in the x-axes direction, the horizontal. Also, restriction supports in the direction of the y-axes, the vertical, were added in the bottom surface of the lower box to impede its movement in that direction. Fig. 4 presents the simulated computer model according to the boundary conditions of the interface shear test.

For the simulation of a constant confining tension as in the physical model, it is applied a punctual load in the center of the steel plate in the top shear box. Due to the high stiffness of the steel plate, the loading is assumed to be distributed uniformly in the sample surface. For the numerical modeling of this effect, it was simulated a material with a 1 mm thickness, corresponding to a liner element with fairly high stiffness (Teixeira et al., 2007).

The side walls of the box were simulated in a similar way. The interface between the steel plates from the top and the sides of the box were simulated as being unlinked, in order for the loading to be applied solely on the underflow. Besides,

to induce the sliding surface, the top and bottom boxes were spaced by 0.1 mm. Fig. 4b) illustrates in details the boundary conditions of the model described.

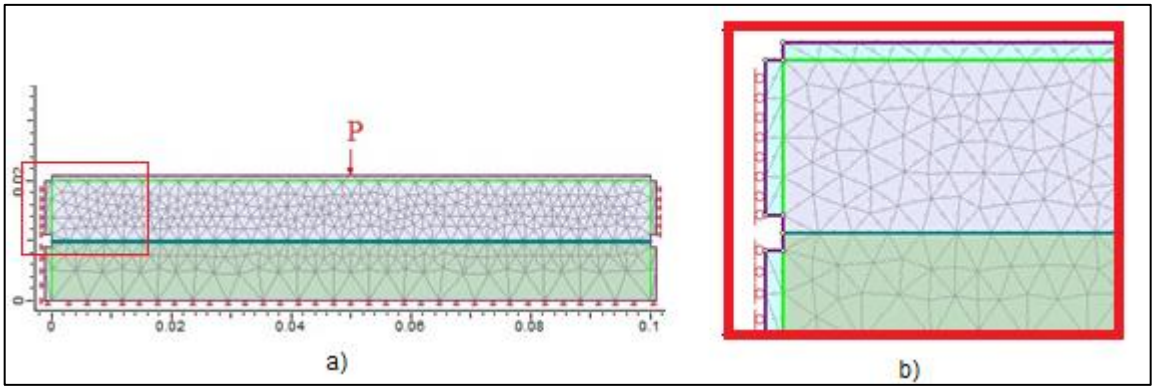

Fig. 4. Boundary conditions of the interface shear test a) shear box; b) detail

The materials presented in this paper, as well as its respective resistance and stiffness parameters, were defined according to the constitutive models adopted for each of the materials.

For this analysis, the steel was simulated according to a linear elastic constitutive model. The geomembrane was modeled according to the elastic-plastic behavior, using the deformability values obtained by Sampaio (Sampaio, 2013) in traction tests. For the underflow and its interface with the geomembrane it was adopted the elastic-linear model, with a constant modulus of deformability.

The structural interface between these two materials was simulated in the *RS2* software as an interface element. For this, firstly the geomembrane was defined as a liner element and, secondly, both its interfaces were defined, the bottom one with the steel plate and the top one with the underflow, by joint elements. In both sides of each joint, it was assumed open nodes as boundary conditions, represented as distinct nodes at the finite element mash and, therefore, can produce relative displacements (ROCSCIENCE, 2017). Fig. 5 displays the lines, with its positive and negative joints and open nodes, as represented in the finite element mesh in the RS2 software.

It is important to notice the limitations of the boundary conditions represented in the model, partly by the unfamiliarity of the behavior of the real model about the sliding in the lower interface of the geomembrane, glued to the steel plate, and the sliding of the lateral interfaces in the walls of the shear box. The influence of these materials' resistance and stiffness in the uncertainties of the numerical analyzes requires more in-depth study and further laboratory testing, therefore not making into this paper. For the glued interface, in order to reduce its influence over the displacements on the geomembrane-underflow studied, since it was glued to the metal in the physical model. So, the resistance parameters of this interface were simulated as being the same used for the steel, and the joints were limited in order to nor have relative displacement between the two materials.

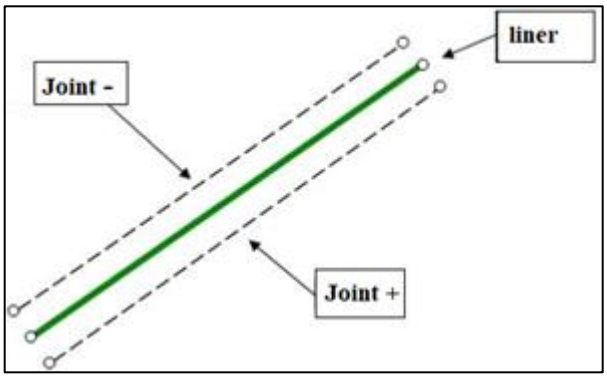

Fig. 5. Liner representation in interface elements by the RS2 Software (ROCSCIENCE, 2017)

Table 2 presents the deformability parameters used in the for the materials and the interfaces. The elasticity model of the interface was considered constant for all the confining tensions defined in the triaxial test done by Sampaio (Sampaio, 2013). The interface's friction angle was determined by the Mohr-Coulomb failure envelope obtained by the interpolation of the pairs of shear stress versus relative displacements values from the interface shear tests (Sampaio, 2013).

The shear modulus of the interface geomembrane-underflow were estimated by the strain-stress deformation obtained for the interface shear test with a confining pressure of 125 kPa, assuming the material as being isotropic and elastic. The same value was then used for the numerical analysis with confining pressures of 500 kPa and 700 kPa.

Table 2. Resistance and Deformability Parameters

Material	φ (°)	E (MPa)	v	f_y (kPa)
Steel	-	200000	0,3	350000
Underflow 95%	36,3	18	0,3	-
Underflow 95%	36,6	18	0,3	-
Interfaces	**φ (°)**	**G (MPa)**	**v**	**f_y (kPa)**
Geomembrane-steel	-	200000	-	350000
Geomembrane-underflow 95%	33	80		

Note: Being φ the friction angle in the Mohr-Coulomb model, E the elastic modulus of the material, G its shear modulus, v its Poisson's ratio and f_y the yielding stress of the steel.

3.2 Loading

After the definition of the model's geometry and the materials, the stages of analysis were defined for different loading stages for which the model would be analyzed. These stages were chosen to simulate a linear increment for relative displacements between the upper and lower boxes. In this, the first stage simulates the boundary conditions before the beginning of the deformations, and the last in the rupture conditions, with displacements of 8 mm or 20% of deformation (Sampaio, 2013), as shown in Fig. 7. Fig. 8 illustrates the application of these displacements and the confining axial stress in the simulated model.

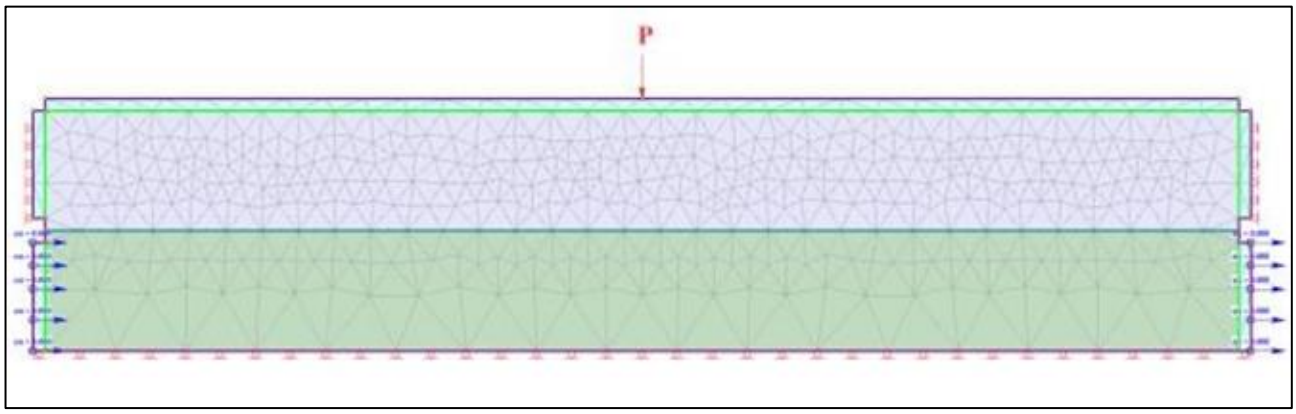

Fig. 7. Loading and displacements introduced in the model at the first stage

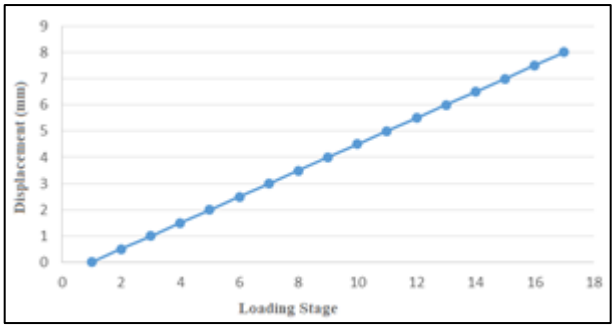

Fig. 8. Relative displacements between the upper and the lower shear box for each simulated loading stages

Fig. 9 a, b and c present the strain-stress charts of the numerical analysis to the three analyzed confining tensions, 125 kPa, 500 kPa and 700 kPa, as well as the comparisons with each respective experimental result.

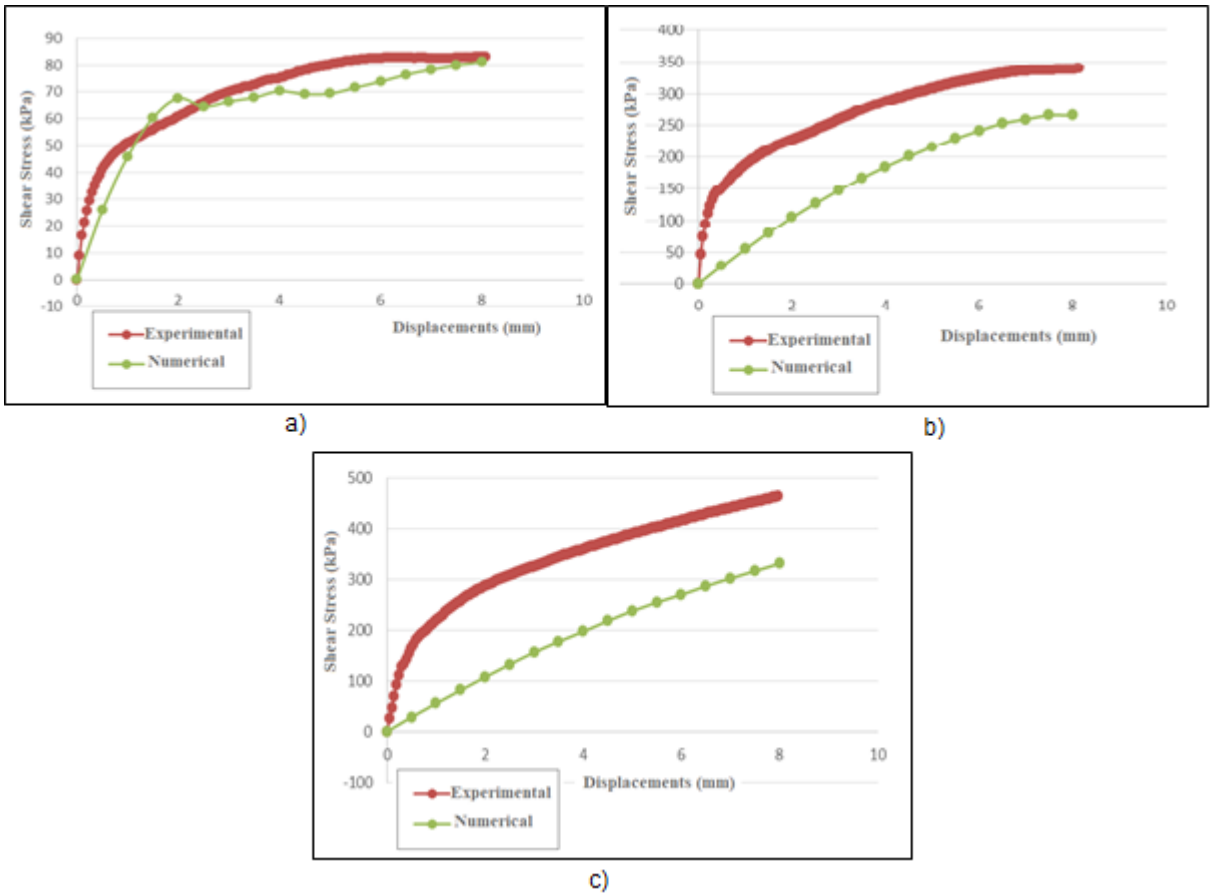

Fig. 9. Comparison between the experimental and numerical stress-strain chart a) confining pressure of 125 kPa; b) confining pressure of 500 kPa; c) confining pressure of 700 kPa;

It can be observed that the numerical results are well fitting to the test data, with a friction angle close to the 33º presented by Sampaio (2013), and a modulus of elasticity of 80MPa. However, for confining tensions higher than 125kPa the simulated curve is presented differs a lot from the respective experimental data. This shows an inadequacy of the model, possibly due to limitations in the modelling or errors in the parameters used for the analysis. It is noted, from the increase of inclination of the experimental curve for higher axial tensions, that the shear stiffness of the interface increases with the confining tension. Therefore, it was sub estimated for the 500 kPa and 700 kPa tests. Regarding the friction angle's adequacy, intimately related to the yield strength of the elastic-perfectly-plastic constitutive model, little can be affirmed for the second and third numerical simulations, once is not possible to account the yielding in these.

In the Fig 10, Fig. 11 and Fig. 12 it presented the shear stress distribution in the section at the last loading stage for all the three confining tensions, 125 kPa, 500 kPa and 700 kPa, respectively. It is also worth noting the geomembrane with its three elements, the upper interface, the liner and the under interface, represented by dashed lines in the colors red, dark blue and green, respectively.

In these figures, it can be seen that the liner did not suffer from yielding in none of the simulations. It can also be seen that, despite the results for the medium shear tension for the loading stages of the interface not showing signs of yielding, for the 500 kPa and 700 kPa simulations the interface yielded in the middle portion of the model. Also, it is noted that in the shear stresses developed in the underflow increase with the increase of the loading, as it is expected. At last, the high shear stresses developed in the left interface in the lower shear box for all the tests could represent the lack of quality of the boundary conditions of the model.

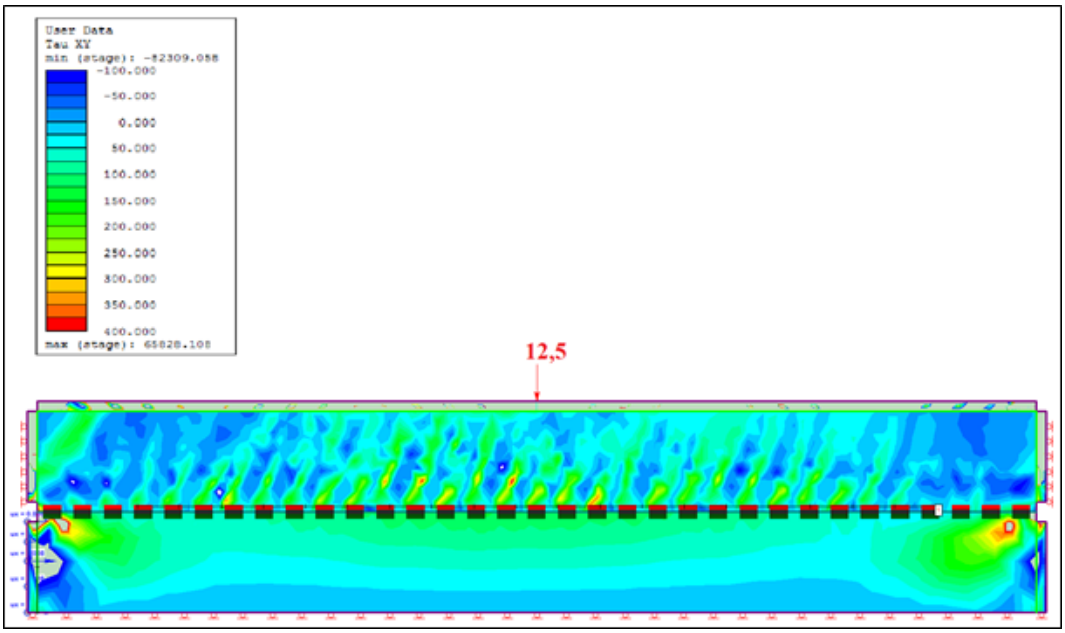

Fig 10. Shear Stresse Diagram in the Section at the Last Loading Stage of the Interface Shear Test with a confining pressure of 125 kPa.

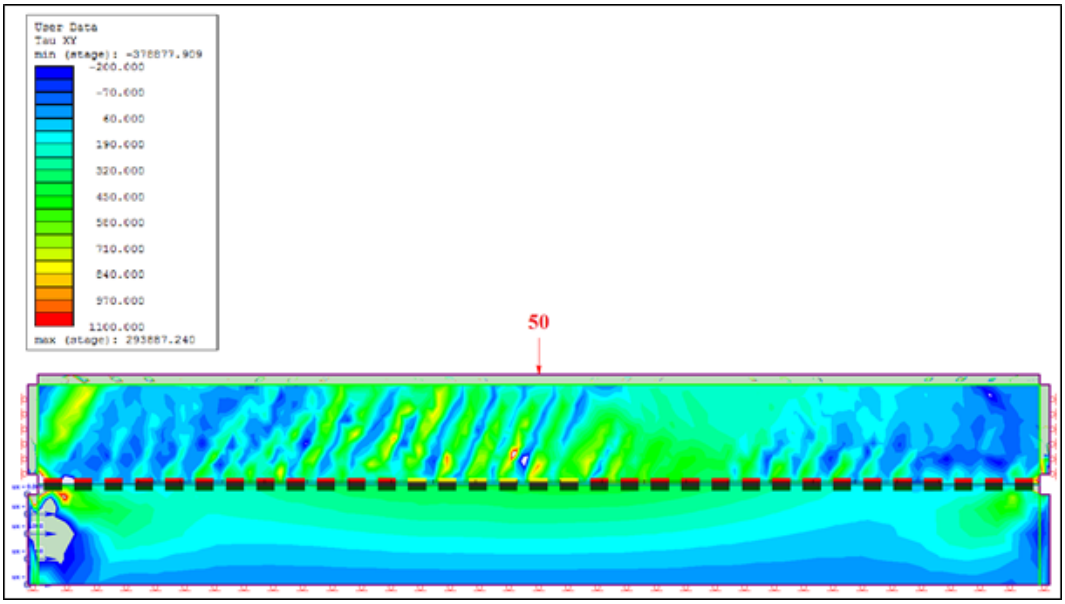

Fig 11. Shear Stress Diagram in the Section at the Last Loading Stage of the Interface Shear Test with a confining pressure of 500 kPa.

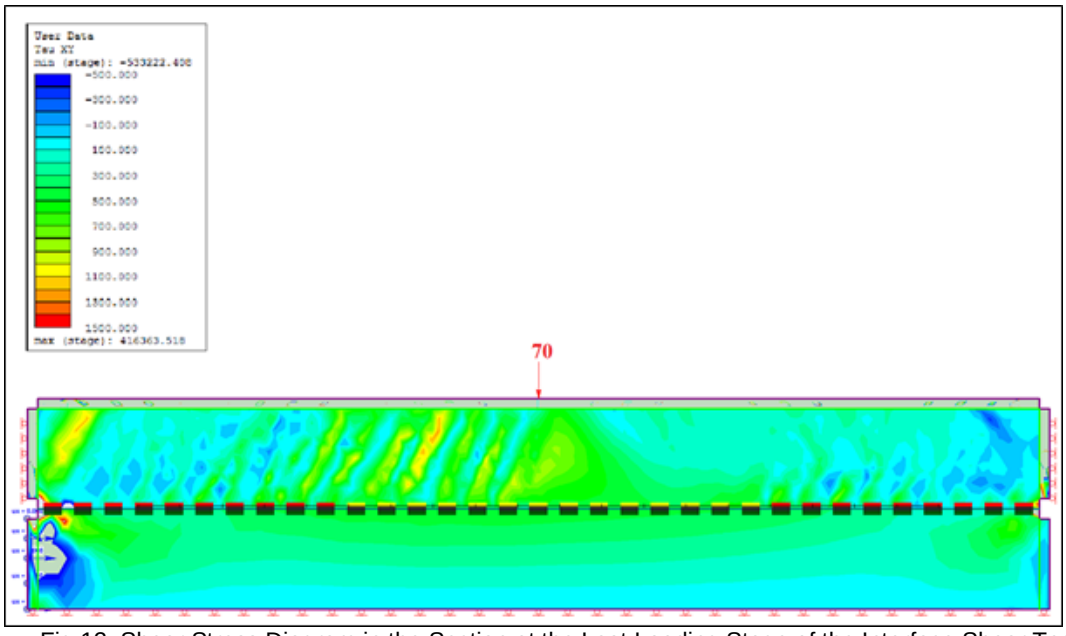

Fig 12. Shear Stress Diagram in the Section at the Last Loading Stage of the Interface Shear Test with a confining pressure of 700 kPa.

The difference between the shear modulus G values that could be estimated using the charts obtained for the 500kPa and 700kPa, in the range of 250MPa. As it was observed that the change in the modulus of elasticity depends on its confining pressure, thus it would be more adequate using a different constitutive model in which this variation could be better described.

Fig. 13 shows the shear stress distribution in the geomembrane-underflow interface along its x-axis. It is observed higher shear stress in the middle of the sample, closer to the point where the axial confining pressure is applied.Furthermore, it can be verified that the tensile solicitation in the geomembrane is very reduces, and it is mobilized 0.042 kPa, less than 1% if the of the HDPE geomembrane residual yield strength, of 700 kPa (Sampaio, 2013). Therefore, it is not observed yielding of the geomembrane in this test. Fig. 14 presents a comparative diagram of the axial forces along the geomembrane x-axis at the last stage of the numerical simulation for the thee confined pressures studied. Here, it can be observed that the low variation of axial forces on the liner for the three simulations, despite the variation of the confining pressures.

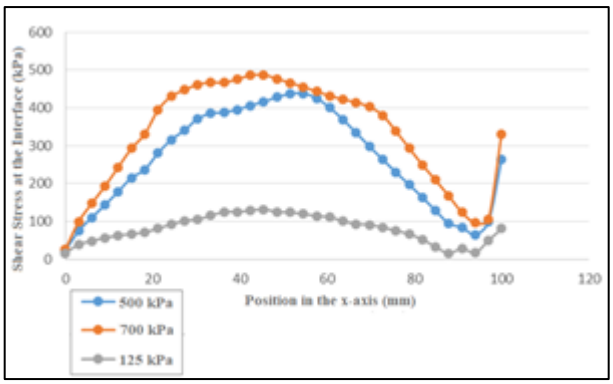

Fig. 13. Shear Stress Distribution at the Interface Geomembrane-Underflow Along its Horizontal Axis

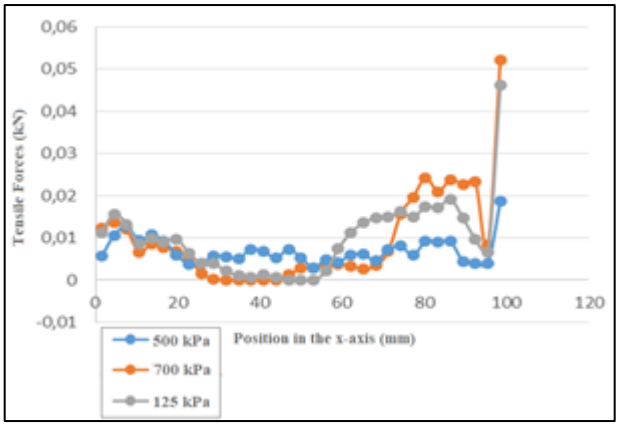

Fig. 14. Tensile Stress Distribution at the Geomembrane Along its Horizontal Axis

4. CONCLUSION

This paper presents a study of the behavior of the interface between a 1.5 mm texturized HDPE geomembrane and cycloned gold ore tailings, under axial and shear loading, in interface shear tests performed by Sampaio (2013).

The interface shear test numerical simulations of the geomembrane-underflow interface were performed using parameters obtained in the literature, as well as parameters interpreted from the experimental data used. The simulated curve has elastic-plastic behavior, and presents a fitting response to the interface shear test experimental data within a range close to an axial loading of 125kPa. However, for higher loadings, the simulations differ from the proposed numerical model, what suggests a need to alter the constitutive model of the interface in order to better describe the loading behavior.

Therefore, further analysis should be made in order to validate the usage of the liner element to simulate the geomembrane, and the interface element to simulate the interface conditions on the interface shear test, and hereafter in the onsite conditions.

5. ACKNOWLEDGEMENTS

The authors want to acknowledge the Federal University of Minas Gerais and Fapemig-Support Foundation of Research of Minas Gerais.

6. REFERENCES

Acosta, L. E. et al., 2018. Displacements Study of an Earth Fill Dam Based on High Precision Geodetic Monitoring and Numerical Modeling. *Sensors*.

Lupo, J. F. & Morrinson, K. F., 2007. Geosynthetic desing and construction approaches in the mining industry. *Geotextiles and Geomembranes*, pp. 96-108.

Power, C. et al., 2017. Five-year performance monitoring of a high density poluethylene (HDPE) cover system at a reclaimed mine waste rock pile in the Sydney COalfield (Nova Scotia, Canada).

ROCSCIENCE, 2017. Slide 4.0: A white paper describing our fully featured limit equilibrium analysis program for slope stability with integrated finite-element groundwater analysis capabilities.

Sampaio, S. S., 2013. *Estudo do Comportamento de Barreiras Poliméricas em Sistemas de Disposição de Rejeito de Minério de Ouro.* Belo Horizonte: Dissertação (Mestrado em Geotecnia e Transportes) - Universidade de Minas Gerais.

Sampaio, S. S., Pimentel, K., Gardoni, M. d. G. & Halabi, A., 2017. *Stability Analysis of a Gold TAilings Dam Lined with HDPE Geomembrane.* Santiago, Chile, s.n.

Teixeira, C. F., 2006. *Análise Numérica de Ensaios em Solo Reforçado com Geogrelhas.* Rio de Janeiro: Dissertação (Mestrado em Engenharia Civil) - Pontifícia Universidade Católica do Rio de Janeiro.

Teixeira, S. H. C., Bueno, B. S. & Zornberg, J. G., 2007. Pullout Resistance of Individual Longitudinal and Transverse Geogrid Ribs. *Journal of Geotechnical and Geoenvironmental Engineering*.

Wijeyesekera, D. C., Siang, A. J. L. M. & Yahaya, A. S. B., 2013. Advanced Statistical Analysis for Relationships between Particle Morphology (Size and Shape) and Shear (Static and Dynamic) Characteristics of Sands. *International Journal of Geosciences*, Volume 4, pp. 27-36.

Yaya, C., Tikou, B. & LiZhen, C., 2017. Numerical analysis and geophysical monitoring for stability assessment of the Northwest tailings dam at Westwood Mine. *International Journal of Mining Science and Technology*.